ELSEVIER

Materials Science and Engineering A 452–453 (2007) 313–320

MATERIALS SCIENCE & ENGINEERING A

www.elsevier.com/locate/msea

Annealing induced oxidation and transformation of Zr thin film prepared by ion beam sputtering deposition

Sung-Wei Yeh [a], Tien-Yu Hsieh [a], Hsing-Lu Huang [b], Dershin Gan [a,*], Pouyan Shen [a]

[a] *Institute of Materials Science and Engineering, National Sun Yat-sen University, Kaohsiung, Taiwan*
[b] *Department of Mechanical Engineering, Chinese Military Academy, Kaohsiung, Taiwan*

Received 26 July 2005; received in revised form 17 October 2006; accepted 18 October 2006

Abstract

Nanocrystalline α-Zr condensates deposited by ion beam sputtering on the NaCl (1 0 0) surfaces and then annealed at 100–750 °C in air. The phases present were identified by transmission electron microscopy to be nanometer-size α-Zr + ZrO, α-Zr + ZrO + c-ZrO_2, c-ZrO_2, c- + t-ZrO_2, t-ZrO_2, and t- + m-ZrO_2 phase assemblages with increasing annealing temperature. The ZrO_2 showed strong {1 0 0} preferred orientation due to parallel epitaxy with NaCl (1 0 0) when annealed between 150 and 500 °C in air. The c- and t-ZrO_2 condensates also showed (1 1 1)-specific coalescence among themselves. The c- and/or t-ZrO_2 formation can be accounted for by the small grain size, the presence of low-valence Zr cation and the lateral constraint of the neighboring grains.

Keywords: Zirconia; Ion beam sputtering; Nanometer; Coalescence; Preferred orientation

1. Introduction

Tetragonal (t-) ZrO_2 polycrystals (TZP) [1] is an alternative of partially stabilized ZrO_2 (PSZ, with t-ZrO_2 precipitates in a cubic (c-) ZrO_2 matrix) [2] or ZrO_2 dispersed ceramic (ZDC, with t-particles embedded in various ceramic host) [3] in which an effective matrix constraint was exerted on t-ZrO_2 crystals for a later beneficial transformation toughening effect of martensitic t- to monoclinic (m-) ZrO_2 transformation [4,5] under stress. Sintering via specific firing schedules or with additives of the space charge effect [6] was conventionally used to prevent the t-ZrO_2 particles from coarsening above a critical size of the t-m transformation [7]. Aerosol or so-called gas evaporation route has been used to produce ultrafine particles of refractory oxides [8] and nanoparticle chain aggregates of titania [9]. This route has never been shown to produce TZP until recently by reactive sputtering on metallic Zr target under various oxygen flow rates [10]. TZP thin layer of nanosize grains formed typically on carbon-coated collodion film [10].

The Zr–ZrO_2 phase diagram [11] relevant to the oxidation of Zr to form TZP film [10] has been well established. In this research, radio frequency (rf) ion beam sputtering on Zr target in vacuum was alternatively used to prepare nanosize Zr thin film and to study the annealing temperature dependence of condensate size and shape, phase identity as well as the way of assembly with respect to the adjoined condensates and the NaCl (1 0 0) substrate. This information is difficult if not impossible to obtain for the condensates overlain on fragile collodion film [10] or using laser ablation on ZrO_2 target in air, as we previously tried on t-ZrO_2 condensates and their (1 1 1)-specific coalescence twinning and martensitic transformation [12].

2. Experimental

Zr target (99.9% pure) was subject to rf ion beam sputtering in order to deposit nanosize Zr thin film on the (1 0 0) surface of NaCl single crystal slabs and glass substrate for subsequent annealing in air at 100, 150, 250, 350, 450, 500, and 750 °C for 1 h. The condensed layer was stripped from NaCl substrate into distilled water, and then mounted on copper grids covered with carbon-coated collodion film for transmission electron microscopic (TEM, JEOL 3010, under 200 and 300 kV.) study. Aperture of 50 μm in diameter was used to take selected area electron diffraction (SAED) patterns. TEM images were taken under bright field image (BFI) and dark field image (DFI) modes using a focal-plane aperture of 10 μm in diameter. The electron

* Corresponding author. Tel.: +886 7 5252000x4054; fax: +886 7 5254099.
E-mail address: dgan@mail.nsysu.edu.tw (D. Gan).

0921-5093/$ – see front matter © 2006 Elsevier B.V. All rights reserved.
doi:10.1016/j.msea.2006.10.131

diffraction patterns of c-, t-, and m-ZrO_2 were indexed according to the distorted c-fluorite cell [13]. Energy dispersive X-ray (EDX) analysis was used for chemical composition determination of the condensates. The EDX analysis was performed using L shell count for Zr and K shell count for O, and the ratio method without absorption correction [14].

Additional experiments with the condensates sputtered on the soda lime glass substrates were employed to study the annealing temperature (100–500 °C for 1 h in air) dependence of the color and translucency changes of the Zr thin film.

3. Results

3.1. Phase identity

The as-prepared thin film consists of α-Zr grains ca. 5–10 nm in size (Fig. 1a). The grains are randomly oriented as indicated by the SAED pattern (Fig. 1b) with no preferred orientation. Fig. 2 shows the SAED patterns of the thin films annealed between 100 and 500 °C in air. The α-Zr transformed to ZrO at 100 °C (Fig. 2a), and to c-ZrO_2 at 150 °C (Fig. 2b) as indicated by the strong (1 1 1) diffraction ring with 0.293 nm d-spacing. The c-ZrO_2 particles have strong preferred orientation as indicated by four diffraction arcs of both {2 0 0} and {2 2 0} (Fig. 2b). The α-Zr and ZrO persist to 200 °C (not shown) but totally transformed to c-ZrO_2 at 250 °C (Fig. 2c). The t-ZrO_2 appeared at 350 °C (Fig. 2d) as indicated by the very weak (1 1 2) ring with a d-spacing of 0.212 nm. The c- + t-ZrO_2 phases persist to 500 °C-1 h annealing as shown in Fig. 2e and f.

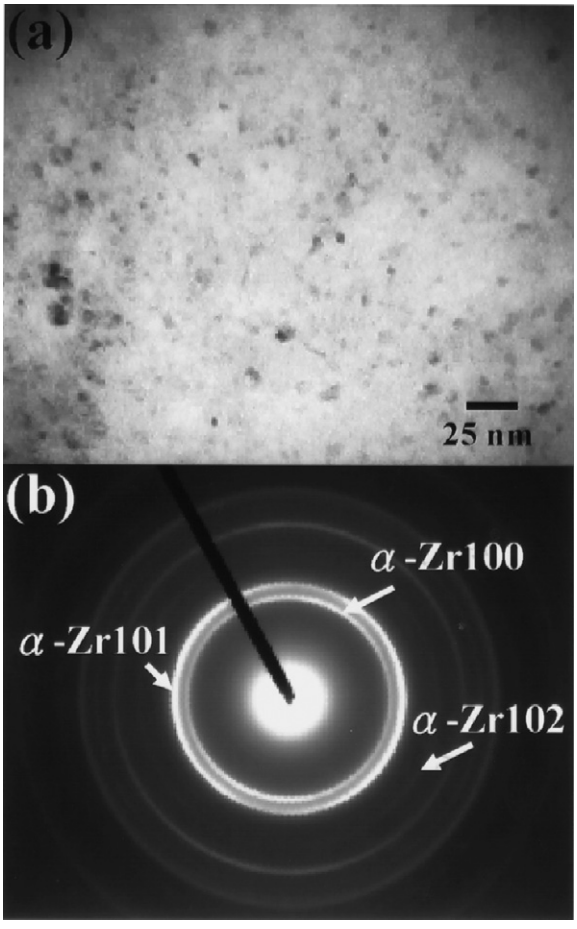

Fig. 1. (a) BFI, (b) SAED pattern of as-prepared thin film on NaCl (1 0 0) with randomly oriented grains ca. 5 nm in size.

Fig. 3a–f are the corresponding BFI of Fig. 2a–f showing that the grain size is 5–10 nm with annealing temperature from 100 to 500 °C with no apparent grain growth. These grains are assembled as mono-grain thick film, as indicated by the absence of Moire fringes (Fig. 3f). The oxidation of α-Zr with increasing temperature leads to the formation of ZrO followed by the c-t transformation. The optimized annealing temperature to form t-ZrO_2 was estimated to be 350–500 °C for 1 h in air.

The t-ZrO_2 partially transformed to m-ZrO_2 at 750 °C as indicated by the sharp (1 1 1) diffraction of m-ZrO_2 (Fig. 4a) and its characteristic twin variants (Fig. 4b). In general, the size of the grains increased to 80 nm at the annealing temperature of 750 °C (Fig. 4b). The m-ZrO_2 particles as large as 50–80 nm in size were recognized by comparing the DFI formed with t-ZrO_2 diffraction only (Fig. 4c), which indicates a t-ZrO_2 grain size up to about 40 nm, and with t- + m-ZrO_2 diffractions together (Fig. 4d). The critical grain size of t-m transformation for undoped ZrO_2 was reported to be 30 nm [7]. The isolated tetragonal ZrO_2 particles larger than this size were therefore vulnerable to martensitic t-m transformation. The arcs in (2 0 0) and (2 2 0) diffractions in Fig. 2 became blurred and the larger particles became faceted upon t-m transformation at 750 °C (Fig. 4a).

EDX analysis indicated the as-deposited α-Zr and subsequently oxidized film (Fig. 5a and b, respectively) have negligible impurities.

3.2. Coalescence

Lattice image of the representative sample annealed at 500 °C for 1 h in air in Fig. 6a shows the {1 0 0} and {1 1 1} faceted c- and/or t-ZrO_2 nanoparticles in the process of coalescence. The (two-dimensional) 2D Fourier transform indicated that these particles were in the [0 1 1] zone axis (Fig. 6b) and coalesced toward the same orientation. The reconstructed image (Fig. 6c) shows that dislocations were left at the interface due to imperfect attachment over vicinal {1 0 0} and/or {1 1 1} contact planes. The same specimen shows also c- and/or t-ZrO_2 nanoparticles in the [0 0 1] zone axis coalesced over {1 0 0} planes (Fig. 7a–c). The (1 0 0) preferred orientation is in accord with the {2 0 0} and {2 2 0} diffraction arcs in Fig. 2f. The {1 1 1}-specific attachment of the c- and/or t-ZrO_2 nanoparticle was also found in another area of the specimens, showing an [$\bar{1}$12] oriented particle coalescing with another particle in ~[0 1 1] zone axis (Fig. 8).

3.3. Translucency of the thin film on glass substrate

The thin film specimens deposited on glass substrate were annealed in air to study the temperature dependence of color and translucency, as shown in Fig. 9. A drastic change of thin film from dark to opal translucent color occurred when annealing temperature was increased from 300 to 350 °C. The dark thin films annealed at lower temperatures have fine surface with low

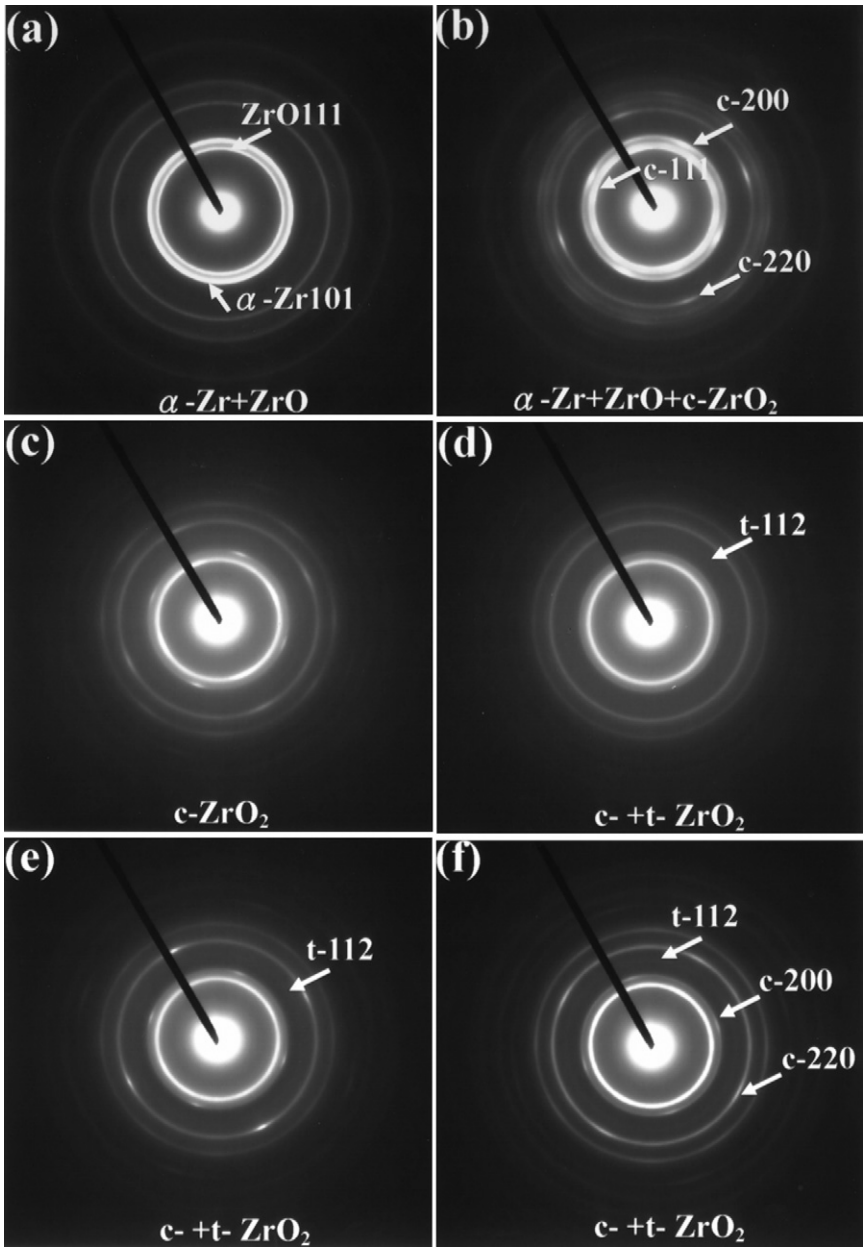

Fig. 2. SAED patterns of the thin films subject to post-deposition annealing at (a) 100 °C, (b) 150 °C, (c) 250 °C, (d) 350 °C, (e) 450 °C, and (f) 500 °C for 1 h showing preferred orientation of ZrO_2 phases due to NaCl (1 0 0) substrate.

roughness and therefore a high reflectivity, as observed under optical reflective light (not shown).

4. Discussion

4.1. Zirconia phase specification

4.1.1. Zr-stabilization effect

Either cations larger than Zr^{4+} in size or cations of divalent or trivalent valences that introduce charge-compensating oxygen vacancies were commonly added to ZrO_2 in considerable amount to form the so-called fully stabilized zirconia (FSZ) with c-fluorite type structure, or in less amount to form PSZ with fine precipitates of t-phase in the c-ZrO_2 matrix [5]. In the present experiment of annealing Zr in air it was found that ZrO was formed at relatively low temperature, i.e., 100–200 °C, indicating the presence of Zr^{2+} ion. These Zr^{2+} ions have lower valence yet larger size than Zr^{4+} ions can therefore stabilize the c- and t-phase. This is supported by the lowering of equilibrium temperature for c/t univariant to about 1490 °C as the extent of ZrO_{2-x} nonstochiometry increases to ca. 64.6 at.% oxygen in the binary Zr–ZrO_2 phase diagram [10] and the fact that the coating on glass substrate is opaque at low annealing temperature and becomes transparent as the annealing temperature is increased to 350 °C. The stabilization of c- and t-ZrO_2 in oxygen deficient condition is also in accord with air annealing results

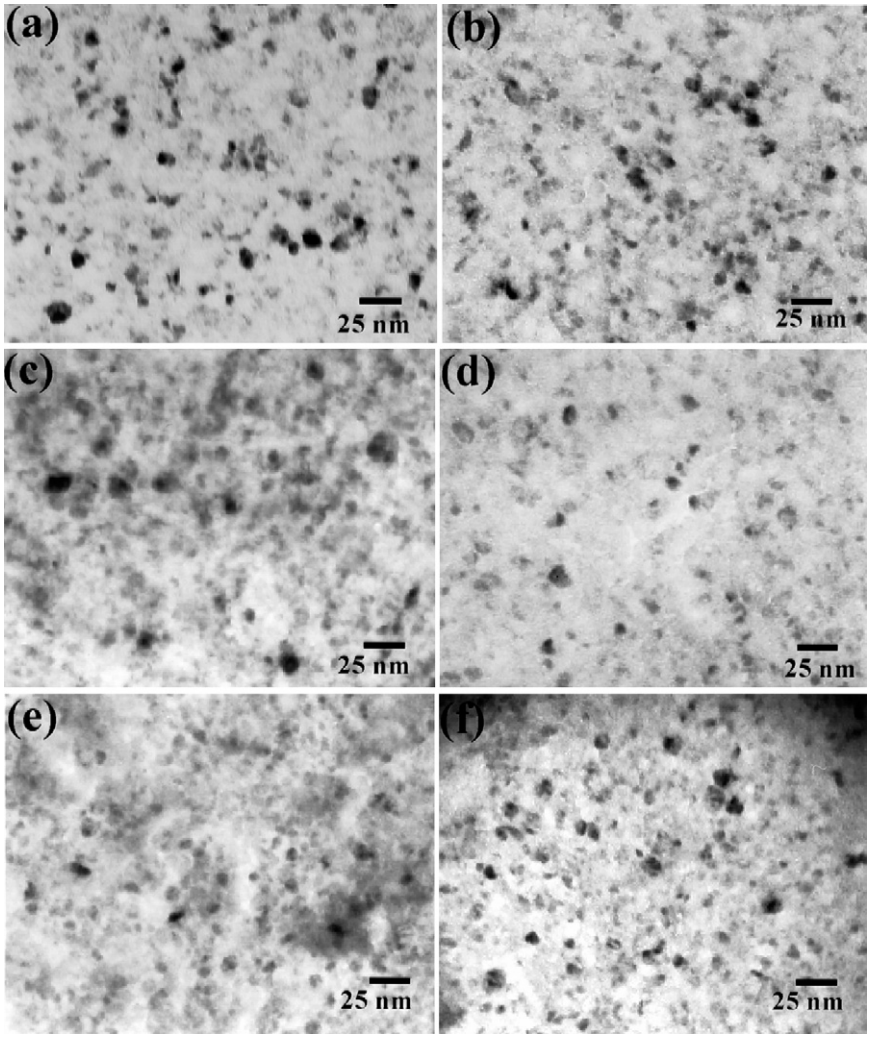

Fig. 3. BFIs of the thin films subject to post-deposition annealing at (a) 100 °C, (b) 150 °C, (c) 250 °C, (d) 350 °C, (e) 450 °C, (f) 500 °C for 1 h showing slightly larger grain size at a higher temperature. Note the absence of Moiré fringes indicates that the films are mono-grain thick.

of the thin zirconia film, which indicated the t-m transformation was lowered by about 150 °C if oxygen vacancies are present [15].

The thin films subject to annealing above 350 °C for 1 h in air became translucent. This is because that oxygen deficient ZrO_2 became stoichiometric c- and/or t-ZrO_2 besides the effect of a better sintering/coalescence of the assembled particles on the glass substrate.

4.1.2. Size and matrix constraint effect

Garvie [7] originally suggested that pure t-ZrO_2 could be stabilized to room temperature due to crystallite size effect. Based on the observations of individual particles precipitated from hydrothermal solution, he estimated the critical size of t-m transformation of isolated tetragonal particles prepared from this wet route is about 30 nm. The present estimation on the condensate route is about 50 nm. The critical size is larger in the case of zirconia particles with an effective matrix constraint, e.g., around 1 μm at room temperature when embedded in ceramic matrices [16]. The nucleation of m-ZrO_2 from t- or orthorhombic ZrO_2 [17] is further facilitated by the presence of dislocations for either constraint [18,19] or non-constraint ZrO_2 particles [12,17] of relatively large size.

The t-m transformation is exothermic and the stabilizing effect by the crystal size is due to the surface energy difference between the t- and m-ZrO_2 crystallites [7]. The t-m transformation of ZrO_2 is accompanied by a volume expansion [3–5], and therefore any constraint that works against the volume expansion can also effectively hinder the t-m transformation and stabilize the t-ZrO_2 phase. In bulk ZrO_2 nanomaterial the surrounding grains can exert a 3D matrix constraint [16] that resists the volume expansion of t-m transformation and stabilizes the t-ZrO_2 grains, as mentioned above. In the present case of thin film ZrO_2 of nanosize grains, in addition to the surface energies, the neighboring grains can exert a 2D constraint that can also help to stabilize the t-ZrO_2 grains. The critical size of t-m transformation was reported to be 80 nm for thin evaporated ZrO_2 film prepared by evaporating the metals in vacuum ($\sim 10^{-4}$ Torr) on NaCl or mica and then stripped for further annealing in vacuum or in air [15]. The larger critical size was attributed to grain-boundary energy effect, although the effect of 2D constraint was not mentioned [15].

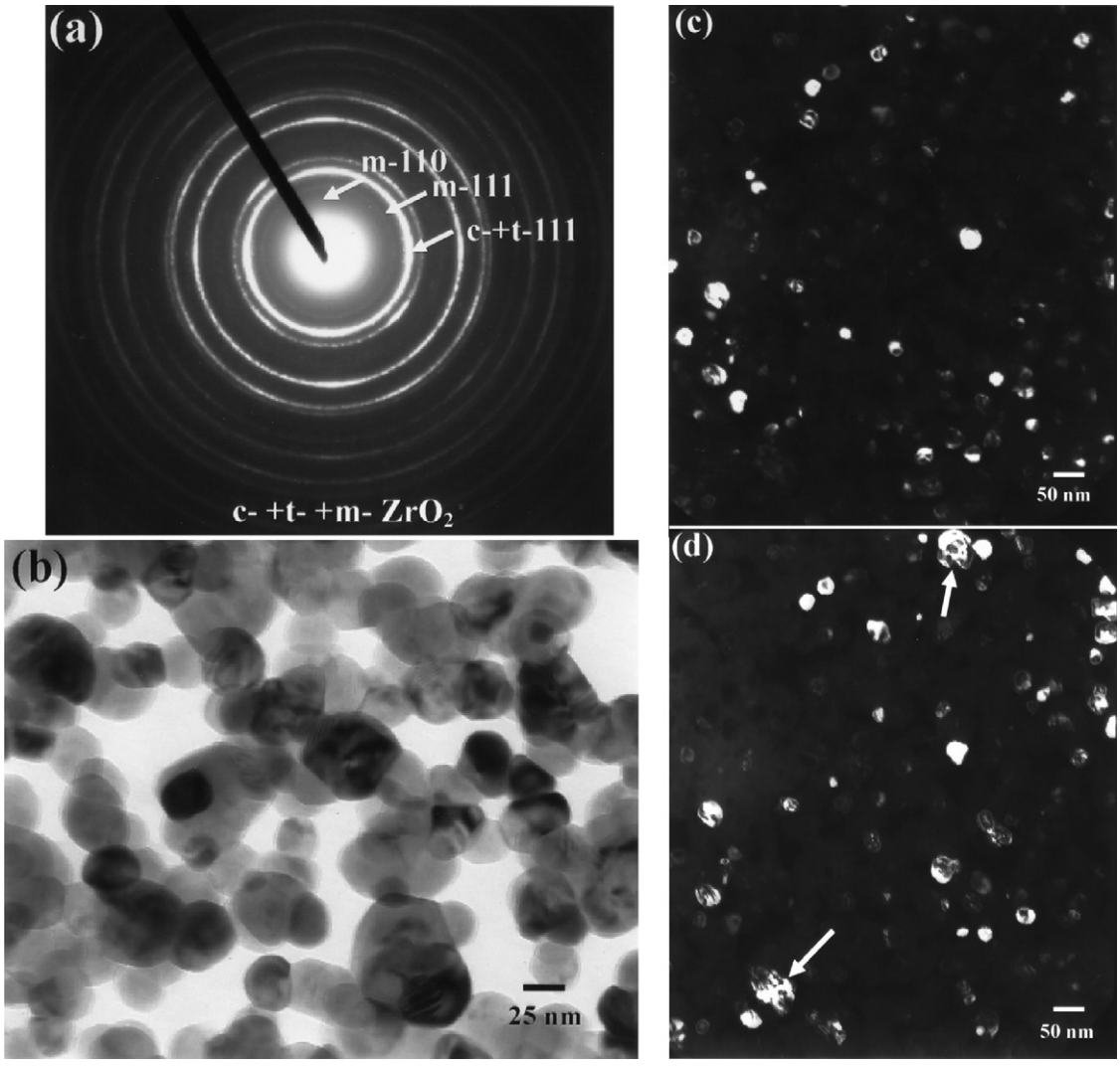

Fig. 4. (a) SAED pattern and (b) BFI of the thin films subject to annealing at 750 °C for 48 h to form much larger sized m-ZrO_2 (>50 nm) from t-ZrO_2, (c) DFI of t-ZrO_2 using (1 1 1) diffraction, (d) DFI of t-ZrO_2 and m-ZrO_2 using (1 1 1) of both phases, showing m-ZrO_2 particles exceeding 50 nm in size (arrowed).

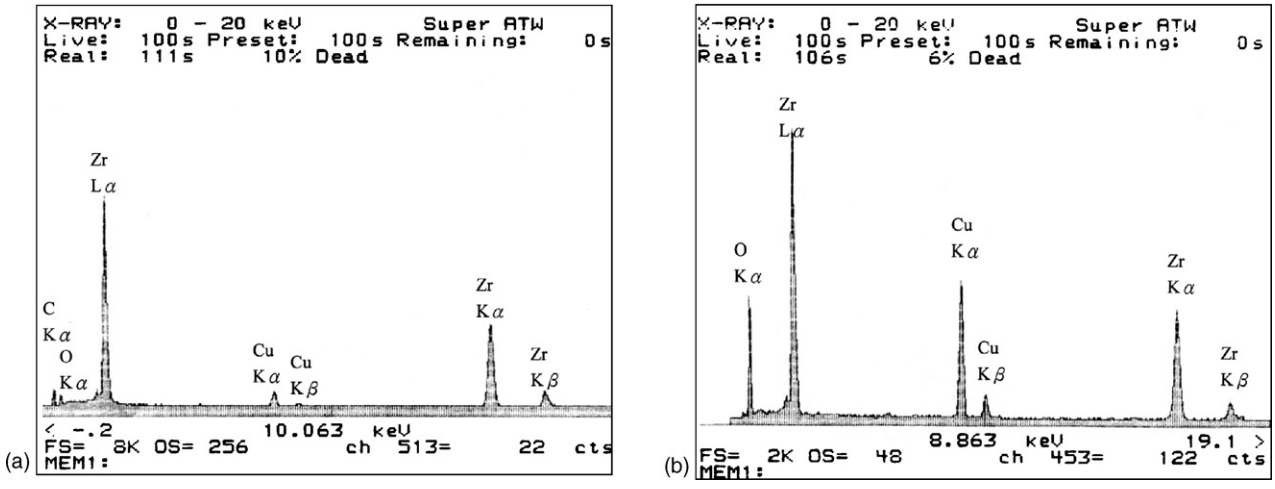

Fig. 5. EDX spectrum of (a) as deposited α-Zr, and (b) ZrO_2, represented by the sample annealed at 250 °C for 1 h in air.

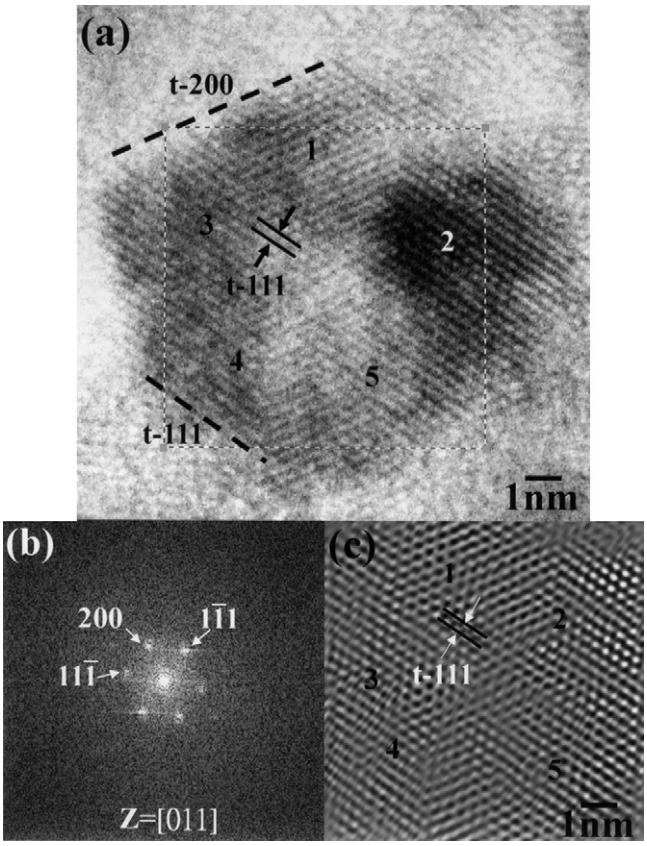

Fig. 6. (a) Lattice image (b) Fourier transformation from the square region in (a) showing {1 0 0} and {1 1 1} faceted c- and/or t-ZrO_2 nanocrystals in nearly [0 1 1] zone axis in the process of coalescence upon annealing at 500 °C for 1 h. (c) The Inverse Fourier transform formed by selecting the diffraction spots in (b) showing dislocations left at the imperfectly impinged interface.

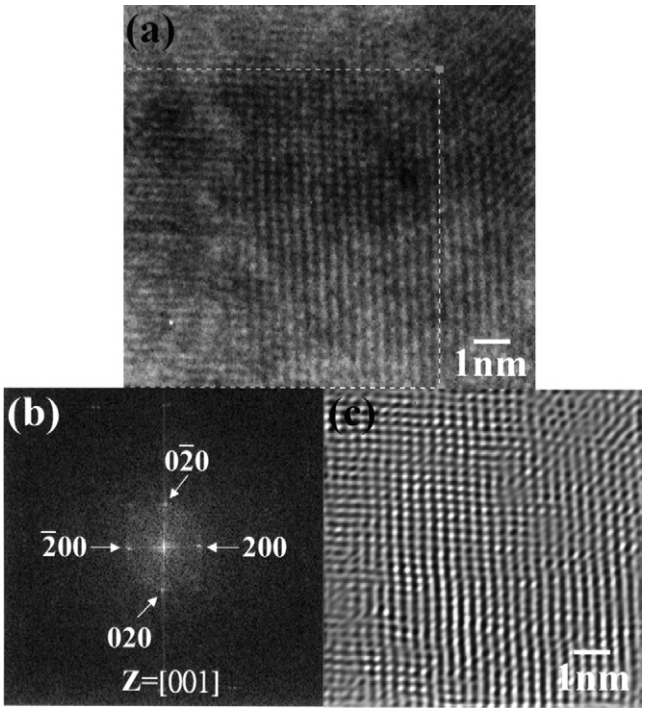

Fig. 7. (a) Lattice image and (b) Fourier transform from the square region in (a) showing that the c- and/or t-ZrO_2 nanocrystals are coalescing in nearly [0 0 1] zone axis upon annealing at 500 °C for 1 h. (c) Inverse Fourier transform showing dislocations at the impinged surface.

4.2. Energetics

4.2.1. Zirconia coalescence

Nanocrystalline particles may grow by reorientation and attachment at specific crystallographic surfaces between adjacent particles. Sometimes a small misorientation may retain among themselves, and dislocations can be formed, as observed for the c- and/or t-ZrO_2 in Figs. 6–8. Coherence may then be achieved by distortion in some areas of the interface, and edge dislocation formed in the regions of step sites, analogous to the observed attachment of titania in hydrothermal solution [20]. Coalescence of fluorite-type condensates over {1 1 1} surface may cause twinning, as observed for CeO_2 condensates [21] and t-ZrO_2 condensates prepared via laser ablation [12]. This is consistent with the oriented attachment of faceted anatase nanocrystals to form twin [22] or single crystal with defects and fault [20].

In the present case, many deposited crystallites were observed to coalesce over (1 1 1) plane, presumably the lowest energy plane. The (*h k l*)-specified attachment/coalescence has been reported for dioxide condensates with underlying reoriented mechanism of Brownian motion of particles [23]. Certain rotation of the crystallites is obviously necessary because the possibility that the crystallites were formed with aligned (1 1 1) planes is quite low. Coalescence may also occur on irrational contact plane or ∼(1 1 1) vicinal surface (Fig. 8). Under such circumstance, considerable atom diffusion across structural ledges is required. The rotation was possible for crystallites with small enough orientation difference in (1 1 1) planes and small enough crystallite size for the Brownian motion to activate the rotation and then the surface energy may carry out the subsequent final coalescence. For crystallites with larger size or larger orientation differences, the rotation is more difficult as in a deposited polycrystalline coating with considerable thickness. Heating the substrate can increase the Brownian motion and facilitate the rotation, but it also increases the rate of coalescence so that individual crystallites may become difficult to distinguish. Since Brownian type rotation is responsible for the orientation change of the condensates as discussed above, a certain amount of rotation energy must be overcome. In addition to surface energy, strain energy must also be consumed to certain extent during coalescence of the present zirconia condensates, in view of the elastic interaction between small nuclei [24].

4.2.2. ZrO_2 condensates over NaCl (1 0 0)

The c-ZrO_2 and/or t-ZrO_2 condensates were found to have {1 0 0} preferred orientation, presumably with respect to NaCl {1 0 0} following parallel epitaxial relationship because the (2 0 0) and (2 2 0) diffraction arcs remained fixed in orientation relative to the removed substrate. It is formed by the rotation of zirconia condensates with preferred orientation with respect to the NaCl crystallographic direction is presumably to lower the interfacial energy, rather than the atom-by-atom epitaxial depo-

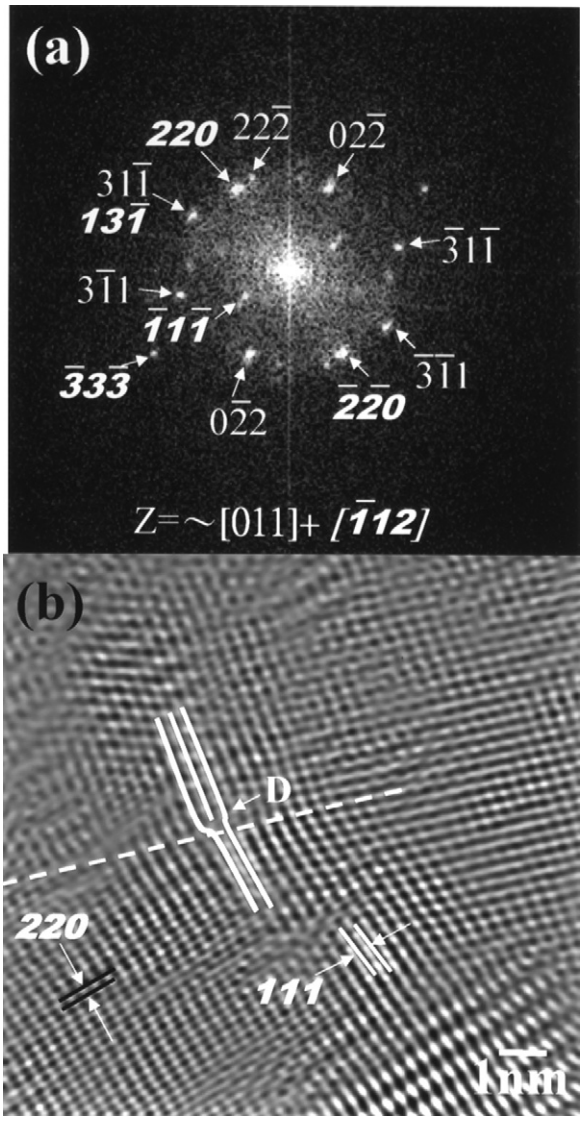

Fig. 8. (a) Fourier transform (b) reconstructed image showing {1 1 1}-specific coalescence of an [$\bar{1}$12] oriented (italic (hkl)) particle with another particle (upright (hkl)) close to the [0 1 1] zone axis. A dislocation, as indicated, is formed at the boundary indicated by a dashed line. The specimen is the same as in Figs. 5 and 6.

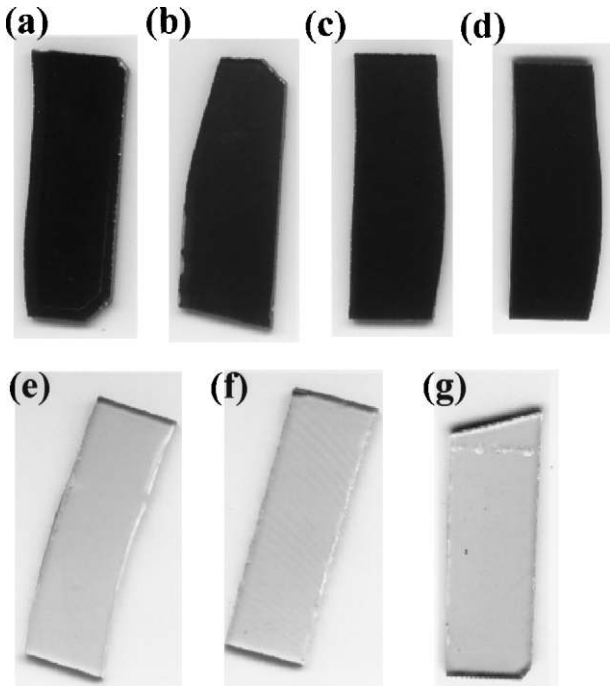

Fig. 9. Photograph showing color and translucency changes of the thin films deposited on glass substrate at different annealing temperature for 1 h (a) 100 °C, (b) 150 °C, (c) 250 °C, (d) 300 °C, (e) 350 °C, (e) 450 °C, and (f) 500 °C. Note the drastic change from dark to opal translucent color occurred from 300 to 350 °C.

sition on the substrate [25]. The effects of particles size, shape and mobility at a specified substrate temperature are important factors. In this regard, fcc metal crystallites have been observed to migrate-rotate [26] and coalesce [27] on the free surface of a single crystal substrate [28]. In addition, theory based on Einstein's theory of Brownian type motion and Eyring's transition state model [27,29], in accordance with experimental results, suggests that rotation of the crystallites may proceed by 'viscous' diffusion of atoms along the interphase interface rather than the free surface. In general, a critical temperature of anchorage release must be reached so that the crystallites can rotate or move under a frictional force related to interfacial viscosity [27,29]. This effect accounts for the orientation change of the accumulated CeO_2 [30] and TiC [31] condensates on amorphous substrate to reach so-called artificial epitaxy. In the present case of parallel epitaxial c- and/or t-ZrO_2 on NaCl (1 0 0), the (1 0 0) interface indeed has a small coincidence site lattice [32]. The randomly deposited α-Zr condensates and the intermediate ZrO were rapidly oxidized to ZrO_2 and such a thermal oxidation process may somehow facilitate Brownian motion of the particles.

5. Conclusions

1. The zirconia condensates deposited by ion beam sputtering and annealed with increasing temperature from 100 to 750 °C for 1 h in air were identified by TEM to be nanometer-size α-Zr + ZrO, α-Zr + ZrO + c-ZrO_2, c-ZrO_2, c- + t-ZrO_2, t-ZrO_2, and t- + m-ZrO_2 assemblages.
2. The optimized temperature to form TZP is between 350 and 500 °C for 1 h in air.
3. The isolated particles with cubic and tetragonal lattice were under 50 nm. The stabilization can be due to the small grain size, low-valence Zr cations, and possibly by the lateral strain of neighboring grains.
4. The zirconia condensates showed strong {1 0 0} preferred orientation due to parallel epitaxy with NaCl (1 0 0) when annealed between 150 and 500 °C in air. The c- and t-ZrO_2 condensates also showed (1 1 1)-specific coalescence among themselves. Brownian rotation of the condensates was suggested to be facilitated by thermal oxidation process for lower surface energy as well as strain energy.
5. The thin films undergone annealing above 350 °C for 1 h became translucent because oxygen deficient c-ZrO_2 trans-

formed to stoichiometric c- and/or t-ZrO_2, and the particles were better sintered/coalesced.

Acknowledgments

This research was supported by National Science Council, Taiwan, ROC under contract NSC93-2120-M-110-001, and partly by Center for Nanoscience and Nanotechnology at NSYSU.

References

[1] T.K. Gupta, J.H. Bechtold, R.C. Kuznicki, L.H. Cadoff, B.R. Rossing, J. Mater. Sci. 12 (1977) 2421.
[2] G.K. Bansal, A.H. Heuer, J. Am. Ceram. Soc. 58 (1975) 235.
[3] N. Claussen, in: N. Claussen, M. Rühle, A.H. Heuer (Eds.), Science and Technology of Zirconia, II, Advances in Ceramics, vol. 12, The American Ceramic Society, Columbus, Ohio, 1984, p. 325.
[4] R.C. Garvie, R.H.J. Hannink, R.T. Pascoe, Nature 258 (1975) 703.
[5] D.J. Green, R.H.J. Hannink, M.V. Swain, Transformation Toughening of Ceramics, CRC Press, Inc., 1989, pp. 1–232.
[6] S.L. Hwang, I.W. Chen, J. Am. Ceram. Soc. 73 (1990) 3269.
[7] R.C. Garvie, J. Phys. Chem. 69 (1965) 1239.
[8] M. Kato, Jpn. J. Apply. Phys. Part 1 15 (1976) 757.
[9] S.K. Friedlander, H.D. Jang, K.H. Ryu, Apply. Phys. Lett. 72 (1998) 173.
[10] I.M. Chen, S.W. Yeh, S.Y. Chiou, D. Gan, P. Shen, Thin Solid Films 491 (2005) 339.
[11] R. Ruh, H.J. Garrett, J. Am. Ceram. Soc. 50 (1967) 257.
[12] P. Shen, W.H. Lee, Nano Lett. 1 (12) (2001) 707.
[13] G. Teufer, Acta Crystall. 15 (1962) 1187.
[14] D.B. Williams, Practical Analytical Electron Microscopy in Materials Science, Philips Electronic Instruments Inc., Mahwah, 1984.
[15] I.A. El-Shanshoury, V.A. Rudenko, I.A. Ibrahim, J. Am. Ceram. Soc. 53 (1970) 264.
[16] M. Rühle, E. Bischoff, N. Claussen, in: H.I. Aaronson, D.E. Laughlin, R.F. Sekerka, C.M. Wayman (Eds.), Solid-Solid Phase Transformations, Metallurgical Society of AIME, Warrendale, PA, 1982, p. 1563, and references cited therein.
[17] Y.H. Chiao, I.W. Chen, Acta Metall. Mater. 38 (1990) 1163.
[18] I.W. Chen, Y.H. Chiao, in: A.H. Heuer, L.W. Hobbs (Eds.), Science and Technology of Zirconia in Advances in Ceramics, vol. 12, American Ceramic Society, Columbus, OH, 1984, p. 33.
[19] I.W. Chen, Y.H. Chiao, Acta Metall. 31 (1983) 1627.
[20] R.L. Penn, J.F. Banfield, Science 281 (1998) 969.
[21] W.S. Lee, P. Shen, J. Crystal Growth 205 (1999) 169.
[22] R.L. Penn, J.F. Banfield, Am. Mineral. 83 (1998) 1077.
[23] L.Y. Kuo, P. Shen, Surf. Sci. 373 (1997) L350–L356.
[24] J.C. Zanghi, J.J. Métois, R. Kern, Surf. Sci. 52 (1975) 556.
[25] D. Walton, J. Chem. Phys. 37 (1962) 2182.
[26] A. Masson, J.J. Métois, R. Kern, Surf. Sci. 27 (1971) 463.
[27] J.J. Métois, M. Gauch, A. Masson, R. Kern, Surf. Sci. 30 (1972) 43.
[28] J.J. Métois, Surf. Sci. 36 (1973) 269.
[29] R. Kern, A. Masson, J.J. Métois, Surf. Sci. 27 (1971) 483.
[30] L.Y. Kuo, P. Shen, Mater. Sci. Eng. A 277 (2000) 258.
[31] L.Y. Kuo, P. Shen, Mater Sci. Eng. A 276 (2000) 99.
[32] S.W. Yeh, H.L. Huang, D. Gan, P. Shen, J. Cryst. Growth 289 (2006) 690.